Effect of Slip Flow on the Steady-State Performance of Aerostatic Porous Journal Bearings

K. C. Singh[1]
Research Scholar.

N. S. Rao
Assistant Professor.

B. C. Majumdar
Professor.

Department of Mechanical Engineering,
Indian Institute of Technology,
Kharagpur - 721 302, India

A theoretical solution is presented to predict the steady-state performance characteristics of aerostatic porous journal bearings of finite thickness considering three dimensional flow in the porous media. The analysis takes into account the velocity slip at the film bearing interface by using Beavers-Joseph criterion. Results are presented in dimensionless form for load capacity and mass rate of flow for different operating conditions and bearing dimensions. Solution is also obtained for modified slip velocity conditions and both the results are compared. It is observed that there is no agreement between two models except for few values of slip parameters. Hence, it is preferable to use the Beavers-Joseph model in order to account for all values of slip parameters. The effect of slip velocity on the static characteristics is discussed.

Introduction

Today, porous bearings are gradually being adopted for industrial applications owing to their better performance and damping characteristics compared to conventional hole-admission bearings [1]. Until recently, in the analyses of such bearings, the investigators were customarily assuming the conventional adherence condition at the porous boundary [2]. Beavers and Joseph [3] proposed an empirical slip velocity boundary condition based on experimental investigations. They predicted the presence of a nonzero tangential velocity, the so-called slip velocity, for the free fluid which is proportional to the shear rate at the porous boundary. In a subsequent work [4], further experimental results were presented showing good correlation with their earlier prediction [3]. Saffman [5] provided theoretical justification using a statistical approach. Taylor [6] and Richardson [7], in companion papers, experimentally and analytically investigated a Couette-type flow bounded by a model permeable material. Excellent agreement was found to prevail between the results from the slip model and those of experiment.

The slip boundary condition of Beavers and Joseph involves an experimentally determined coefficient, the so-called slip coefficient, which is argued to be independent of the properties of fluid. This has also been experimentally verified [4] to be true in case of Poiseuille flows of oil and water. Based on this agrument, the slip boundary condition has widely been employed by investigators [8–10] in the analyses of oil bearings. However, no investigations on the applicability of slip-flow model for compressible lubricants were being reported till 1974, when beavers et al. [11] justified the validity through experimental verification with gaseous lubricants.

Sparrow et al. [12] in their analyses with incompressible fluids, used the slip boundary condition in a slightly modified form neglecting the contribution of Darcy's velocity components at the bearing interface. Following this, Wu and Castelli [13, 14] provided steady state solutions for self-acting porous gas bearings. Rao [15] studied the effect of slip flow on the performance of aerostatic journal bearings with thin bushes using the modified slip velocity boundary conditions. However, Prakash and Vij [9] observed some considerable difference in the values of load capacity predicted using the two slip velocity boundary conditions [3, 12].

In the present analysis, steady-state solution has been obtained for journal bearings with compressible lubricant considering the Beavers-Joseph criterion [3], hitherto to be referred as the full slip boundary condition, at the bearing interface. Solution has also been obtained by using the modified slip boundary condition [12] for different values of slip coefficient α and permeability factor σ, for the sake of comparison. The differential equation governing the flow in the porous media and the modified Reynolds' equation for the flow in the bearing clearance are solved simultaneously for pressure distribution in the bearing clearance. Load capacity and mass rate of flow are computed for different supply pressures and bearing dimensions, with respect to the bearing feeding parameter.

The comparison of the results for the conventional no-slip condition, obtained from the present analysis as a special case, with the similar available theoretical and experimental results [16] shows a good agreement.

Analysis

Figure 1 shows a schematic diagram of a porous journal

[1] On study leave from University College of Engineering, Burla - 768 018, Orissa, India.

Contributed by the Lubrication Division for publication in the JOURNAL OF LUBRICATION TECHNOLOGY. Manuscript received by the Lubrication Division, June 28, 1982.

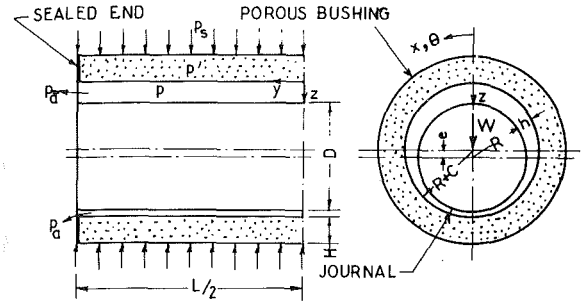

Fig. 1 Schematic diagram of an externally pressurized porous gas journal bearing

bearing with an impermeable stationary journal of radius R. The porous material is assumed to be homogeneous and isotropic. The ends of the porous bushing are sealed to prevent end leakage. Compresseo air is fed, at a constant pressure p_s, from behind the bushing throughout the length of the bearing. The pressure drops to p' in the porous matrix, then to p in the bearing clearance and finally the lubricant exhausts to the atmosphere at a pressure p_a.

Governing Equation for Pressure in the Porous Media. The velocity components in the porous matrix are u', v', and w', and are given by Darcy's law.

$$u' = -\frac{k}{\eta}\frac{\partial p'}{\partial x} \tag{1}$$

$$v' = -\frac{k}{\eta}\frac{\partial p'}{\partial y} \tag{2}$$

$$w' = -\frac{k}{\eta}\frac{\partial p'}{\partial z} \tag{3}$$

The steady-state continuity equation for compressible lubricants is given by

$$\frac{\partial(\rho u')}{\partial x} + \frac{\partial(\rho v')}{\partial y} + \frac{\partial(\rho w')}{\partial z} = 0 \tag{4}$$

Substituting for velocity components from equations (1)–(3) and assuming the flow to be isothermal everywhere and the gas obeys the equation of state.

$$p = \rho \mathcal{R} T \tag{5}$$

the governing equation for the flow of the gas can be written as

$$\frac{\partial^2 p'^2}{\partial x^2} + \frac{\partial^2 p'^2}{\partial y^2} + \frac{\partial^2 p'^2}{\partial z^2} = 0 \tag{6}$$

Modified Reynolds' Equation. The governing differential equation for pressure in the lubricating film can be derived starting from Navier-Stokes equations (neglecting the effect of inertia force compared to the viscous force) and taking into account,

(*a*) the mass exchange of the lubricant between the bearing-matrix and the film region, and

(*b*) the velocity slip occurring at the film-bearing interface.

The Navier-Stokes equations for the problem are

$$\frac{\partial^2 u}{\partial z^2} = \frac{1}{\eta}\frac{\partial p}{\partial x} \tag{7}$$

$$\frac{\partial^2 v}{\partial z^2} = \frac{1}{\eta}\frac{\partial p}{\partial y} \tag{8}$$

$$\frac{\partial p}{\partial z} = 0 \tag{9}$$

The corresponding boundary conditions are

(*i*) at $z = 0$ (interface)

$$\frac{\alpha}{k^{1/2}}[u(x,y,0) - u'l(x,y,0)] = \frac{\partial u}{\partial z} \tag{10}$$

$$\frac{\alpha}{k^{1/2}}[v(x,y,0) - v'(x,y,0)] = \frac{\partial v}{\partial z} \tag{11}$$

$$w(x,y,0) = w'(x,y,0) \tag{12}$$

where, $u(x, y, 0)$ and $v(x, y, 0)$ are slip velocities

and α = slip coefficient, a dimensionless quantity depending on the characteristics of permeable material but independent of the properties of fluid [4, 11].

Equations (10)–(12) are the full-slip boundary conditions applicable to the bearing interface as proposed by Beavers and Joseph [3].

The above slip-boundary conditions as expressed in a slightly modified form, neglecting the effect of Darcy's components [12] are

Nomenclature

C = radial clearance
D = diameter of journal
e = eccentricity
$G, \bar{G}$ = mass rate of flow, $\bar{G} = \dfrac{24\eta\mathcal{R}TG}{C^3(p_s^2 - p_s^2)}$ (dimensionless)
$h, \bar{h}$ = film thickness, $\bar{h} = h/C$ (dimensionless)
H = thickness of the porous bushing
k = permeability of the porous material
L = length of the bearing
$p, \bar{p}$ = pressure (absolute) in the film, $\bar{p} = p/p_a$
p_a = ambient pressure (absolute)
$p_s, \bar{p}_s$ = supply pressure (absolute), $\bar{p}_s = p_s/p_a$
$p', \bar{p}'$ = pressure (absolute) in the bearing matrix, $\bar{p}' = p'/p_a$
Q, Q' = modified pressures $Q = \bar{p}^2$, $Q' = \bar{p}'^2$
R = radius of journal
$\mathcal{R}$ = universal gas constant
T = absolute temperature of gas
u, v, w = components of velocity along x, y, and z directions in the lubricating film
u', v', w' = components of velocity along x, y, and z directions in the porous matrix
$W, \bar{W}$ = load capicity, $\bar{W} = \dfrac{W}{LD(p_s - p_a)}$ (dimensionless)
x, y, z = cartesian coordinates
$\theta, \bar{y}, \bar{z}$ = $\theta = x/R$, $\bar{y} = y/(L/2)$, $\bar{z} = z/H$
α = slip coefficient
$\beta = \dfrac{12kR^2}{C^3H}$, feeding parameter (dimensionless)
$\epsilon = e/C$, eccentricity ratio (dimensionless)
η = absolute viscosity of gas
ρ = density of gas
θ = angular coordinate
$\sigma = \dfrac{C}{k^{1/2}}$, permeability factor (dimensionless)

$$\frac{\alpha}{k^{1/2}}u(x,y,0)=\frac{\partial u}{\partial z} \tag{13}$$

$$\frac{\alpha}{k^{1/2}}v(x,y,0)=\frac{\partial v}{\partial z} \tag{14}$$

$$w(x,y,0)=w'(x,y,0) \tag{15}$$

(*ii*) at $z = h$ (journal surface)

$$u(x,y,h)=0 \tag{16}$$

$$v(x,y,h)=0 \tag{17}$$

$$w(x,y,h)=0 \tag{18}$$

(*iii*) at $z = 0, p = p'$ (19)

i.e., the pressure across the interface is continuous.

Integrating equations (7) and (8) with the boundary conditions for both the interface (equations (10) and (11)) and the journal surface (equations (16) to (18))

$$u(x,y,z)=\frac{1}{2\eta}\frac{\partial p}{\partial x}(z-h)\left(z+\frac{2k+hk^{1/2}/\alpha}{k^{1/2}/\alpha+h}\right) \tag{20}$$

$$v(x,y,z)=\frac{1}{2\eta}(z-h)\left(z+\frac{2k+hk^{1/2}/\alpha}{k^{1/2}/\alpha+h}\right) \tag{21}$$

Substituting equations (20) and (21) into the continuity equation and integrating over the film thickness, one obtains

$$\frac{\partial}{\partial x}\left\{\frac{h^3}{12\eta}\left(1+\frac{3}{h}\frac{2k+hk^{1/2}/\alpha}{k^{1/2}/\alpha+h}\right)\frac{\partial p^2}{\partial x}\right\}+$$

$$\frac{\partial}{\partial y}\left\{\frac{h^3}{12\eta}\left(1+\frac{3}{h}\frac{2k+hk^{1/2}/\alpha}{k^{1/2}/\alpha+h}\right)\frac{\partial p^2}{\partial y}\right\}=\frac{k}{\eta}\frac{\partial p'^2}{\partial z}\Big|_{z=0} \tag{22}$$

Equation (22) is the modified Reynolds' equation governing the flow in the bearing clearance and satisfying the full slip boundary conditions [3].

With the following substitutions

$$\theta=x/R,\bar{y}=y/(L/2),\bar{z}=z/H,\bar{h}=h/C,Q=(p/p_a)^2,$$

$$Q'=(p'/p_a)^2,\beta=\frac{12kR^2}{C^3H}\text{ and }\sigma=\frac{C}{k^{1/2}},$$

equations (6) and (22) when written in nondimensional form are,

$$\frac{\partial^2 Q'}{\partial\theta^2}+\left(\frac{D}{L}\right)^2\frac{\partial^2 Q'}{\partial\bar{y}^2}+\left(\frac{R}{H}\right)^2\frac{\partial^2 Q'}{\partial\bar{z}^2}=0 \tag{23}$$

$$\frac{\partial}{\partial\theta}\left\{\bar{h}^3(1+\xi_1)\frac{\partial Q}{\partial\theta}\right\}+\frac{\partial}{\partial\bar{y}}\left\{\bar{h}^3(1+\xi_1)\frac{\partial Q}{\partial\bar{y}}\right\}\left(\frac{D}{L}\right)^2$$

$$=\beta\frac{\partial Q'}{\partial\bar{z}}\Big|_{\bar{z}=0} \tag{24}$$

where

$$(1+\xi_1)=\frac{4+\bar{h}\alpha\sigma}{1+\bar{h}\alpha\sigma}+\frac{6\alpha}{\sigma\bar{h}(2+\bar{h}\alpha\sigma)} \tag{25}$$

The modified Reynolds' equation, considering the modified slip boundary conditions (equations 13 and 14) will be same as equation (24) except for the slip factor $(1 + \xi_1)$ which reduces to:

$$(1+\xi_1)=\frac{4+\bar{h}\alpha\sigma}{1+\bar{h}\alpha\sigma} \tag{26}$$

In this case, since the parameters α and σ appear as a product, they together can be considered as a single parameter [13–15]. However, α and σ are to be considered separately when the full-slip boundary conditions are applied. This is evident from equation (25).

Boundary conditions

(*i*) $0\le\theta\le2\pi,0\le\bar{y}\le1$ and $\bar{z}=-1;\bar{p}'=\bar{p}_s$(Supply condition)

(*ii*) $0\le\theta\le2\pi,0\le\bar{y}\le1$ and $\bar{z}=0;\bar{p}=\bar{p}'$(Continuity condition)

(*iii*) $0\le\theta\le2\pi,\bar{y}=1$ and $0<\bar{z}\le-1;\frac{\partial\bar{p}'}{\partial\bar{y}}=0$ (sealed end condition)

(*iv*) $0\le\theta\le2\pi,\bar{y}=0$ and $0\le\bar{z}\le-1;\frac{\partial\bar{p}'}{\partial\bar{y}}=0$ (symmetry condition)

(*v*) $\theta=0$ and $\pi,0\le\bar{y}\le1$ and $0\le\bar{z}\le-1;\frac{\partial\bar{p}'}{\partial\theta}=0$ (symmetry condition)

(*vi*) $0\le\theta\le2\pi,\bar{y}=1$ and $\bar{z}=0;\bar{p}=1$ (ambient condition) (27)

Method of Solution. The governing equations (23) and (24) are linear in Q and solved simultaneously for pressure distribution in the bearing clearance satisfying the appropriate boundary conditions (equation (27)). Since a closed form solution is not possible, the solution is obtained numerically using the finite difference method. A three-dimensional grid pattern is adopted with i, j, and k directions along x, y, and z axes, respectively (Fig. 1). Equations are used in cartesian form which amounts to unwrapping the bearing in the same manner as the film. It has been shown that the curvature effect can be neglected even for higher values of H/R ($H/R = 0.4$), for the values of the permeability coefficient usually encountered in practice [17]. Equations (23) and (24) are written in finite difference form, using central difference quotients for second order derivatives and three point backward difference quotients for first order derivatives, and solved by iteration with a successive over-relaxation (SOR) scheme on a digital computer. Due to symmetry along the length as well as the circumference (at $\theta = 0$ and π) only one quarter of the bearing is considered. The convergence criterion employed is

$$\left|\frac{\Sigma Q^{n+1}-\Sigma Q^n}{\Sigma Q^{n+1}}\right|\le0.001$$

where n = no. of iterations.

Bearing Characteristics. The steady state characteristics are assessed from its load capacity and mass flow rate.

1. Load capacity:

It is expressed as

$$W=-4\int_0^{\pi}\int_0^{L/2}p\cos\theta\,R\,dy\,d\theta \tag{28}$$

in dimensionless form

$$\bar{W}=\frac{W}{LD(p_s-p_a)}$$

$$=-\frac{1}{(\bar{p}_s-1)}\int_0^{\pi}\int_0^{1}\bar{p}\cos\theta\,d\bar{y}\,d\theta \tag{29}$$

2. Mass Rate of Flow. The mass rate of flow is calculated from the volume of the gas flowing out at two ends of the bearing.

$$G=4\int_0^{h}\int_0^{\pi}\rho v\,R\,d\theta\,dz \tag{30}$$

Substituting for v from equation (20), it reduces to

$$G=-4\int_0^{\pi}\frac{\rho h^3}{12\eta}\frac{\partial p}{\partial y}\left(1+\frac{3}{h}\frac{2k+hk^{1/2}/\alpha}{k^{1/2}/\alpha+h}\right)R\,d\theta \tag{31}$$

When simplified

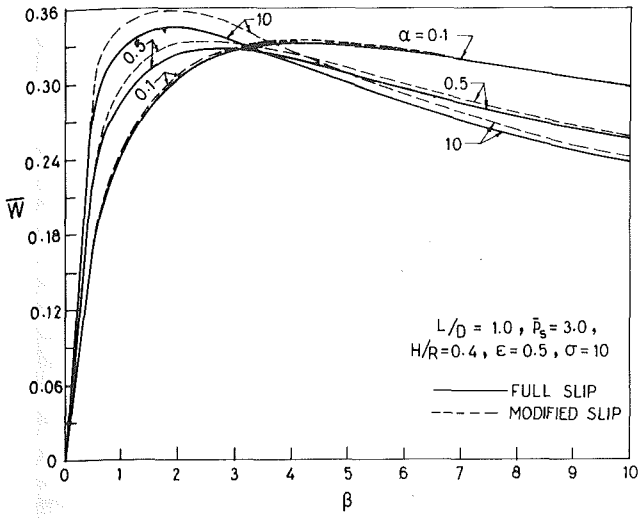

Fig. 2 Load capacity $\bar{W}$ versus feeding parameter β for different values of slip coefficient α

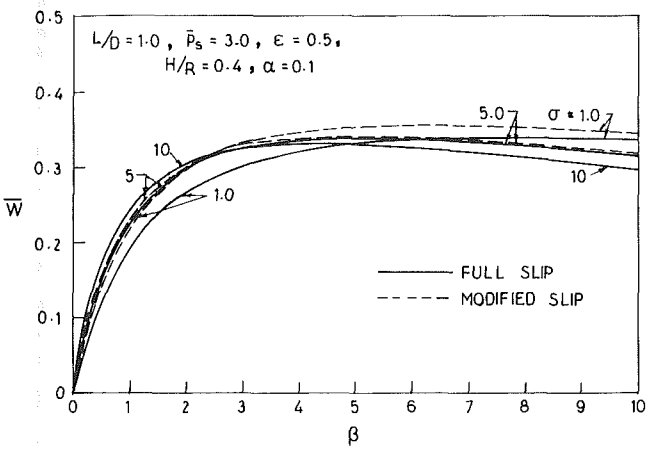

Fig. 3 Load capacity $\bar{W}$ versus feeding parameter β for different values of permeability factor σ

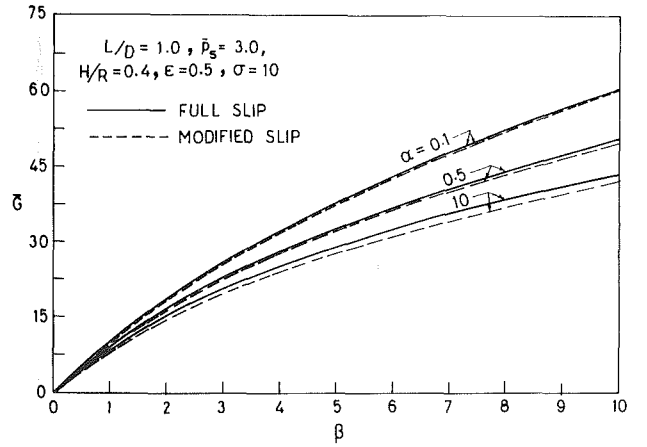

Fig. 4 Mass rate of Flow $\bar{G}$ versus feeding parameter β for different values of slip coefficient α

$$G = -\frac{4C^3 p_a^2}{24\eta \Re T}\left(\frac{D}{L}\right)\int_0^{\pi}\frac{\partial Q}{\partial \bar{y}}\Big|_{\bar{y}=1}\bar{h}^3(1+\xi_1)d\theta \quad (32)$$

Let $\bar{G} = \dfrac{24\eta \Re T G}{C^3(p_s^2 - p_a^2)}$

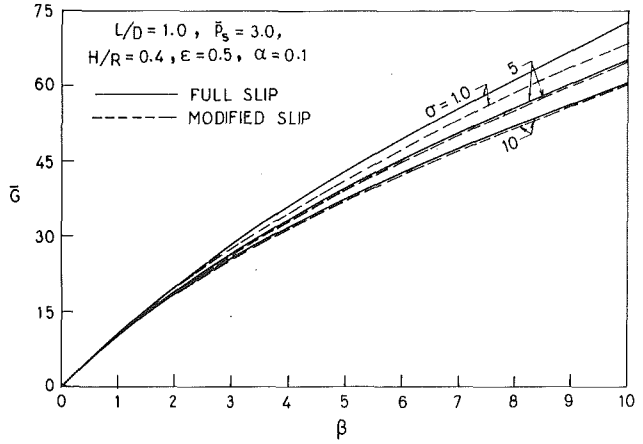

Fig. 5 Mass rate of flow $\bar{G}$ versus feeding parameter β for different values of permeability factor σ

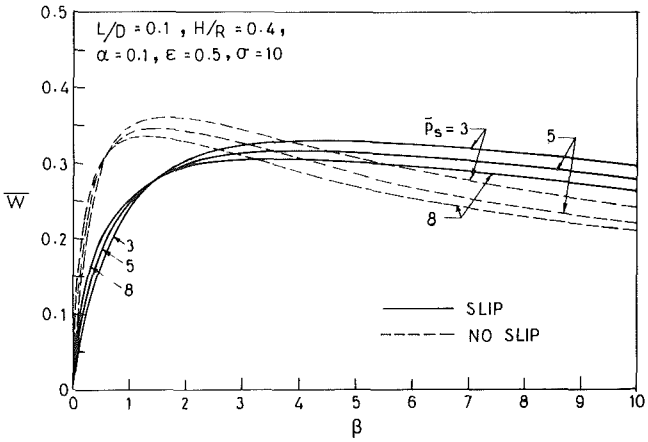

Fig. 6 Load capacity $\bar{W}$ versus feeding parameter β for different values of supply pressure $\bar{p}_s$

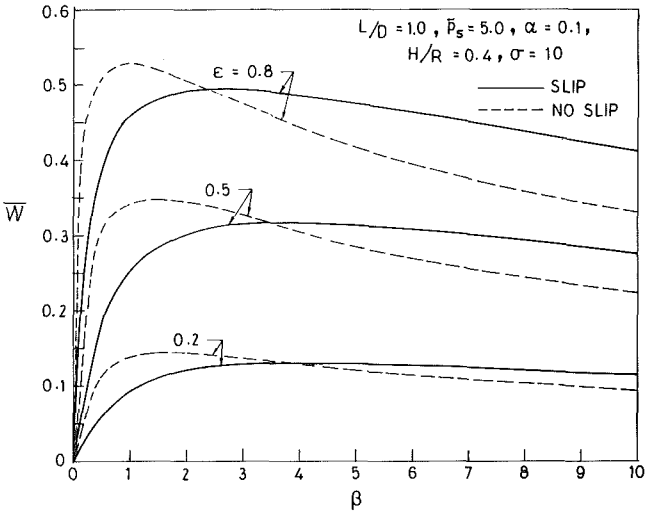

Fig. 7 Load capacity $\bar{W}$ versus feeding parameter β for different values of eccentricity ratio ϵ

So that

$$\bar{G} = -\frac{4}{(\bar{p}_s - 1)}\left(\frac{D}{L}\right)\int_0^{\pi}\frac{\partial Q}{\partial \bar{y}}\Big|_{\bar{y}=1}\bar{h}^3(1+\xi_1)d\theta \quad (33)$$

Results and Discussion

The slip-flow criterion at the porous boundary is taken into

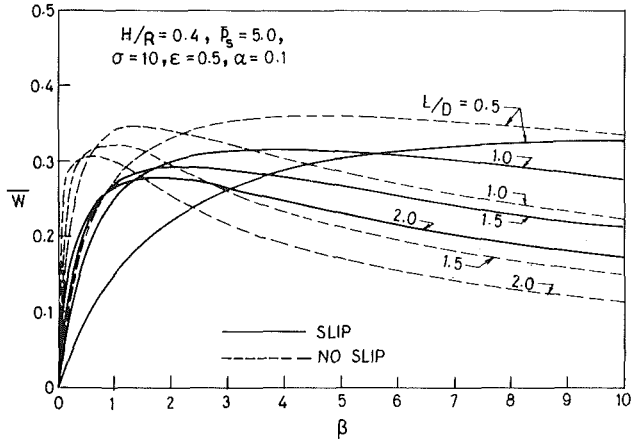

Fig. 8 Load capacity $\bar{W}$ versus feeding parameter β for different values of L/D ratio

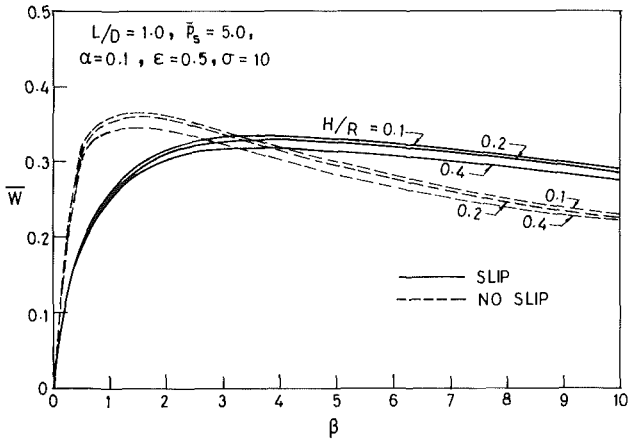

Fig. 9 Load capacity $\bar{W}$ versus feeding parameter β for different values of thickness parameter H/R

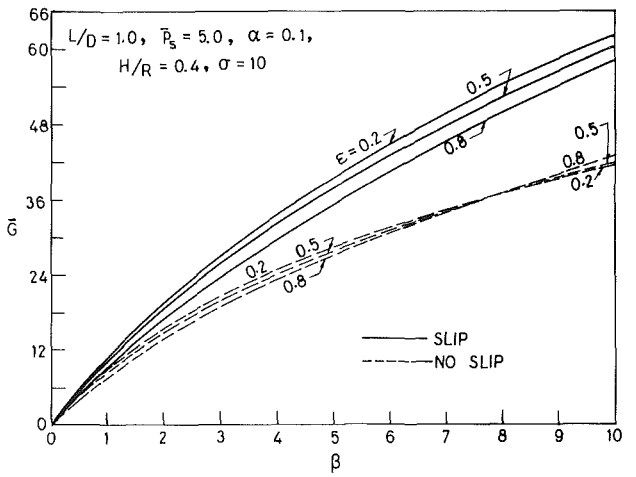

Fig. 10 Mass rate of flow $\bar{G}$ versus feeding parameter β for different values of eccentricity ratio ϵ

account by two independent nondimensional parameters, α and σ, which are related to the properties of the porous matrix. The effect of these parameters on load capacity $\bar{W}$, with respect to feeding parameter β, for both full and modified slip boundary conditions are illustrated in Figs. 2 and 3. Figures 4 and 5 show the corresponding variation in mass rate of flow $\bar{G}$ with β. The variation of $\bar{W}$ with β both

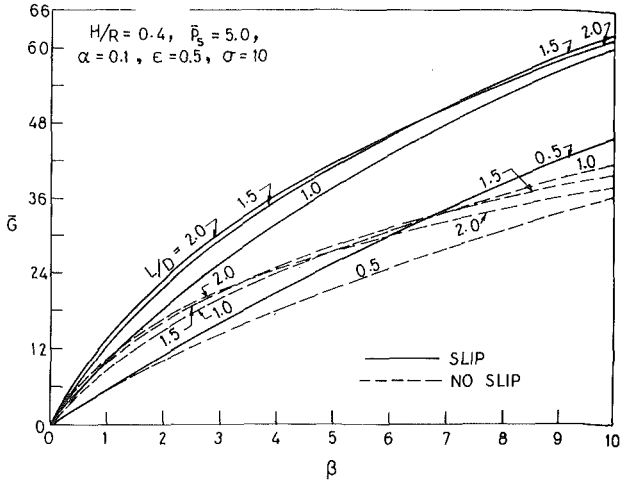

Fig. 11 Mass rate of flow $\bar{G}$ versus feeding parameter β for different values of L/D ratio

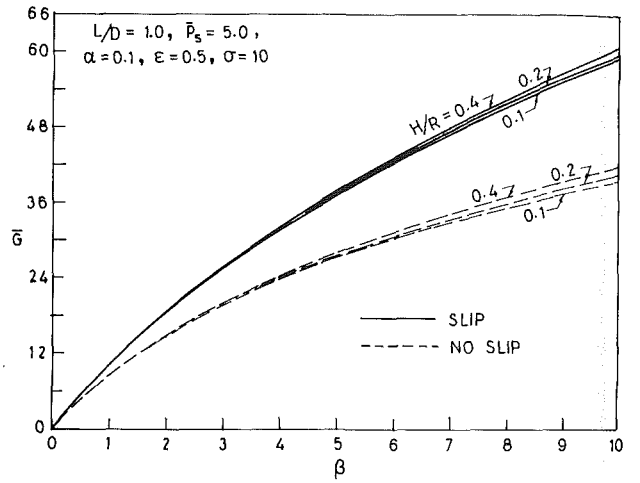

Fig. 12 Mass of flow $\bar{G}$ versus feeding parameter β for different values of thickness parameter H/R

for full-slip and no-slip conditions, and for different supply pressures and bearing dimensions, such as, L/D ratio, thickness parameter H/R, and eccentricity ratio ϵ is presented in Figs. 6–9.

The variation in mass rate of flow $\bar{G}$ with β for different values of ϵ, L/D, and H/R ratio is shown in Figs. 10–12, for both full slip and no-slip conditions. A comparison of the results for the no-slip case with the similar available solution [16] is provided in Fig. 13.

Effect of Slip Parameters α and σ and Comparison Between the Two Slip-Flow Models. Load capacity $\bar{W}$ increases with slip coefficient α in the lower range of feeding parameter β (Fig. 2), whereas, the trend is reversed in the higher range of β. For a value of β around 3.25, variation in α does not seem to have any effect on $\bar{W}$ for the bearing parameters considered in Fig. 2. It is seen that, the rate of change in $\bar{W}$ decreases for higher values of α. The effect of permeability factor σ on $\bar{W}$ is observed to be similar as in case with α (Fig. 3). Mass rate of flow $\bar{G}$ decreases with increase in both α and σ for all values of β (Figs. 4 and 5).

Higher values of load capacity are obtained with modified slip conditions compared to that with full-slip model for all values of α and σ (Figs. 2 and 3). However, the difference in $\bar{W}$ due to the two slip models is negligible for $\alpha = 0.1$ and increases with increase in α (Fig. 2), whereas, maximum

deviation in $\bar{W}$ is obtained for $\sigma = 1.0$, and decreases as σ is increased (Fig. 3). In both the cases, the maximum difference in $\bar{W}$ is obtained in the lower range of β and two values approach each other as β is increased (Figs. 2 and 3). It is seen that, both the slip flow models tend to yield the same result for lower values of α ($\alpha \leq 0.1$) and higher values of σ ($\sigma \geq 5$). This is also evident from the equations (25) and (26), as the values of the slip factor $(1 + \xi_1)$ tends to be the same under the limiting conditions $\alpha \to 0$ and $\sigma \to \infty$, thereby indicating that, the modified slip boundary conditions may be employed for small values of α ($\alpha \leq 0.1$) or higher values of σ ($\sigma \geq 5$). However, it is preferable to adopt the full-slip model, which accounts for all values of α and σ, in order to study the effect of slip on the bearing characteristics. With this view, all other results presented in this paper are based on the full-slip boundary conditions.

Effect of Feeding Parameter (β). Load capacity $\bar{W}$ increases with β, rather sharply in the initial stage ($\beta = 2$ to 3), to attain a maximum and then decreases slowly with further increase in β for all values of supply pressure $\bar{p}_s$, eccentricity ratei ϵ, and bearing dimensions, such as, L/D and H/R ratios (Figs. 6–9). The mass rate of flow $\bar{G}$ increases steadily with β for all values of ϵ, L/D and H/R (Figs. 10–12).

The effect of velocity slip, in general, is to reduce the load capacity $\bar{W}$ in the lower range of β and to increase $\bar{W}$ in the higher range of β for all operating conditions and bearing dimensions when compared with no-slip case (Figs. 6–9). The effect of slip is observed to be more predominant for the value of β corresponding to the maximum load capacity, predicted by no-slip case. Due to the influence of velocity slip, the mass rate of flow $\bar{G}$ increases for all values of β (Figs. 10–12). The effect of slip is also seen to be more predominant at higher values of β.

Effect of Supply Pressure ($\bar{p}_s$). Load capacity increases slightly with $\bar{p}_s$ upto a certain value of β ($\simeq 1.5$) beyond which $\bar{W}$ decreases with increase in $\bar{p}_s$ (Fig. 6). The value of β, for which both the slip and no-slip model predict the same load capacity, decreases slightly with increase in $\bar{p}_s$. The effect of slip on $\bar{W}$ is not influenced much by supply pressure.

Effect of Eccentricity Ratio (ϵ). Load capacity $\bar{W}$ increases appreciably with ϵ (Fig. 7). For lower values of ϵ ($\epsilon = 0.2$) $\bar{W}$ increases with β to a maximum and thereafter maintained almost constant with further increase in β. For higher values of ϵ (0.5 and 0.8) $\bar{W}$ increases rather sharply to attain a maximum value and then decreases slowly with further increases in β. The range of β, in which the conventional adherence condition predicts better load capacity, decreases with increase in ϵ. Mass rate of flow $\bar{G}$ decreases with increase in ϵ (Fig. 10). However, for the no-slip case, the variation of $\bar{G}$ with ϵ is negligible at higher values of β ($\beta = 7$ to 8), beyond which the trend is reversed. The effect of slip is more predominant at higher values of ϵ (Fig. 7).

Effect of L/D Ratio. Load capacity $\bar{W}$, increases slightly with L/D ratio for small values of β ($\beta \simeq 1.5$) beyond which it decreases quite significantly as L/D ratio is further increased (Fig. 8). The range of β, in which the effect of slip is detrimental, reduces with increase in L/D ratio. Mass rate of flow $\bar{G}$ increases with L/D ratio in the lower range of β ($\beta < 7$), whereas, the trend is reversed in the higher range of β (Fig. 11). The effect of slip is slightly more predominant for higher values of L/D ratio.

Effect of Thickness Parameter (H/R). Load capacity $\bar{W}$ remains almost unaffected for lower values of β ($\simeq 1.0$) beyond which it decreases slightly with increase in H/R ratio (Fig. 9). When H/R ratio is decreased to a minimum (say $H/R \leq 0.1$), the bearing behaves as a thin bearing and flow in the porous matrix predominates in the radial direction resulting a better load capacity. Mass flow rate $\bar{G}$ remains unchanged with H/R ratio upto a fairly higher value of β ($\beta \simeq 5$), beyond which a slight increase in flow rate with H/R ratio is observed (Fig. 12).

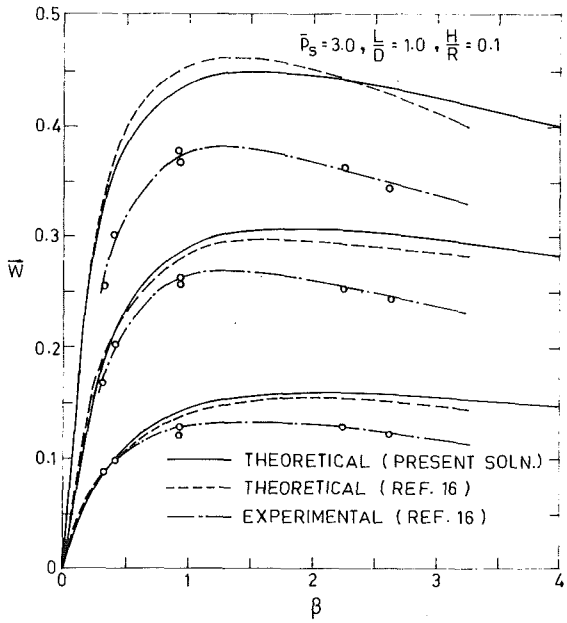

Fig. 13 Comparison of load capacity $\bar{W}$ with the previous solution (no-slip case) (Fig. 5, reference [16])

Comparison With the Previous Results. The solution for the conventional no-slip condition is obtained from the present analysis as a special case (with $\xi_1 = 0$, equation (24)) and the results are compared with the theoretical and experimental results of Sneck and Elwell (Fig. 5, reference [16]) (Fig. 13). Since the previous analysis does not contain a thickness parameter the present results provided for comparison correspond to a minimum value of H/R ($H/R = 0.1$). The results of reference [16] are suitable converted according to the present notations. For smaller eccentricity ratio ($\epsilon = 0.2$), the results are seen to be in good agreement. Slight variation of the present results, with the theoretical results of reference [16], for higher eccentricities ($\epsilon = 0.4$ and 0.6) is expected since the previous results are based on perturbation analysis applicable only for lower eccentricity ratios ($\epsilon < 0.5$).

Summary and Conclusions

The analysis, considering three-dimensional flow in the porous matrix, takes into account the slip velocity at the interface of the porous surface and the bearing clearance. The Beavers-Joseph slip velocity boundary conditions, the so-called full-slip velocity conditions, and the modified slip velocity conditions are compared to study the effect of slip flow on the static characteristics of the bearing.

It is preferable to use the full Joseph-Beavers conditions as there is no agreement between the two models except for very small values of α and very high values of σ. The effect of slip is to reduce the load capacity for low values of β and to increase the load capacity at higher values of β. The mass rate of flow increases with slip for all values of β. It is observed that the effect of slip is more predominant around the value of β, corresponding to the maximum load obtained with the conventional adherence boundary condition. Therefore, while deciding the optimum value of β corresponding to the maximum load capacity, consideration should be given to account for the slip.

References

1 Heller, S., Shapiro, W., and Decker, O., "A Porous Hydrostatic Gas Bearing for Use in Miniature Turbomachinery," *ASLE Trans.*, Vol. 14, No. 2, 1971, pp. 144–155.

2 Majumdar, B. C., "Gas Lubricated Porous Bearings: A Bibliography," *Wear*, Vol. 36, 1976, pp. 269–273.

3 Beavers, G. S., and Joseph, D. D., "Boundary Conditions at a Naturally Permeable Wall," *Journal of Fluid Mechancis*, Vol. 30, Part-I, 1967, pp. 197–207.

4 Beavers, G. S., Sparrow, E. M., and Magnuson, R. A., "Experiments on Couple Parallel Flows in a Channel and a Bounding Porous Medium," ASME *Journal of Basic Engineering*, Vol. 92, No. 4, Dec. 1970, pp. 843–848.

5 Saffman, P. G., "On the Boundary Condition at the Surface of a Porous Medium," *Studies in Applied Mathematics*, Vol. L, No. 2, June 1971, pp. 93–101.

6 Taylor, G. I., "A Model for the Boundary Condition of a Porous Material, Part 1," *Journal of Fluid Mechanics*, Vol. 49, Part II, 1971, pp. 319–326.

7 Richardson, S., "A Model for the Boundary Condition of a Porous Material, Part 2," *Journal of Fluid Mechanics*, Vol. 49, Part II, 1971, pp. 327–336.

8 Murti, P. B. K., "Effect of Slip-Flow in Narrow Porous Bearings," ASME JOURNAL OF LUBRICATION TECHNOLOGY, Vol. 95, No. 4, Oct. 1973, pp. 518–523.

9 Prakash, J., and Vij, S. K., "Analysis of Narrow Porous Journal Bearing Using Beavers-Joseph Criterion of Velocity Slip," ASME *Journal of Applied Mechanics*, Vol. 41, No. 2, June 1974, pp. 348–354.

10 Prakash, J., and Vij, S. K., "Effect of Velocity Slip in Axially Undefined Porous Bearings," *Wear*, Vol. 38, No. 2, July 1976, pp. 245–263.

11 Beavers, G. S., Sparrow, E. M., and Masha, B. A., "Boundary Condition at a Porous Surface which Bounds a Fluid Flow," *AIChE Journal*, Vol. 20, No. 3, May 1974, pp. 596–597.

12 Sparrow, E. M., Beavers, G. S., and Hwang, I. T., "Effect of Velocity Slip on Porous-Walled Squeeze Films," ASME JOURNAL OF LUBRICATION TECHNOLOGY, Vol. 94, No. 3, July 1972, pp. 260–265.

13 Wu, E. R., and Castelli, V., "Gas-Lubricated Porous Bearings—Infinitely Long Journal Bearings, Steady-State Solution," ASME JOURNAL OF LUBRICATION TECHNOLOGY, Vol. 98, No. 3, July 1976, pp. 453–462.

14 Wu, E. R., and Castelli, V., "Gas-Lubricated Porous Bearings—Short Journal Bearings, Steady-State Solution," ASME JOURNAL OF LUBRICATION TECHNOLOGY, Vol. 99, No. 3, July 1977, pp. 331–338.

15 Rao, N. S., "Analysis of Aerostatic Porous Journal Bearings Using the Slip Velocity Boundary Conditions," *Wear*, Vol. 76, No. 2, 1982, pp. 35–47.

16 Sneck, H. J., and Elwell, R. C., "The Externally Pressurized Porous Wall, Gas-Lubricated Journal Bearing II," *ASLE Trans.*, Vol. 8, 1965, pp. 339–345.

17 Rouleau, W. T., and Steiner, L. I., "Hydrodynamic Porous Journal Bearings. Part I—Finite Full Bearings," ASME JOURNAL OF LUBRICATION TECHNOLOGY, Vol. 96, No. 3, July 1974, pp. 346–353.